# $H_\infty$ Gain-scheduled Controller Design for Rejection of Time-varying Disturbances with application to an Active Suspension System

Alireza Karimi and Zlatko Emedi

***Abstract*— A new method for H-infinity gain-scheduled controller design by convex optimization is proposed that uses only frequency-domain data. The method is based on loop shaping in the Nyquist diagram with constraints on the weighted infinity-norm of closed-loop transfer functions. This method is applied to an active suspension system for adaptive rejection of multiple narrow-band disturbances. First, it is shown that a robust controller can be designed for the rejection of a sinusoidal disturbance with known frequency. The disturbance model is fixed in the controller, based on the internal model principle, and the other controller parameters are computed by convex optimization to meet the constraints on the infinity-norm of sensitivity functions. It is shown next that a gain scheduled-controller can be computed for a finite set of disturbance frequencies by convex optimization. An adaptation algorithm is used to estimate the disturbance frequency which adjusts the parameters of the internal model in the controller. The simulation and experimental results show the good performance of the proposed control system.**

## I. Introduction

In control engineering problems, disturbance rejection is an extremely important task. Some disturbances have periodic character and can even be expressed as combination of few sinusoidal signals. Typical examples of systems with periodic disturbances are hard disks [1], optical disk drives [2], helicopter rotor blades [3] and active noise control systems [4].

In the case that the disturbance frequency is known, certain approaches, such as internal model control and repetitive control techniques can be applied. If unknown frequency can be measured directly or indirectly, which happens e.g. in some active noise control applications, adaptive feedforward control can be used for the rejection of disturbance. In [5], it was shown that the standard adaptive feedforward control algorithm is equivalent to the internal model control law. Survey on methods in both cases of known and unknown disturbance frequency can be found in [6].

A linear parameter-varying (LPV) controller design method is described in [7] for rejection of sinusoidal disturbances. In this approach, the controlled system is augmented with LPV model of measurable disturbance in state-space. Then an LPV controller is designed with $H_\infty$ performance based on approach proposed in [8] and [9] using a single quadratic Lyapunov function for all values of measured frequency. A new method for fixed-order LPV controller design with application to disturbance rejection of an active suspension system is proposed in [10]. Although LPV controllers can guarantee the closed-loop stability for fast variation of the scheduling parameters they suffer from poor performance because of their conservatism.

In this paper a fixed-order $H_\infty$ gain-scheduled controller design method based only on the frequency-domain data is proposed. In this method, computation of the controller parameters and their interpolation are performed by one convex optimization as it is proposed in [11]. Then a solution to a challenging benchmark problem [12] for rejection of time-varying narrow-band disturbances is provided using a new toolbox for robust controller design in the frequency domain which is available for free [13].

The paper is organized as follows: Section II describes the gain-scheduled $H_\infty$ controller design method that uses only the frequency response of the model. The method is applied to the benchmark problem for adaptive disturbance rejection of an active suspension system in Section III. Section IV presents the simulation and the experimental results. Finally, Section V gives some concluding remarks.

## II. Gain-scheduled $H_\infty$ controller design

A fixed-order $H_\infty$ controller design method for spectral models is proposed in [14]. In this section we extend this method to design of gain-scheduled $H_\infty$ controllers.

A classical way to design gain-scheduled controllers includes two steps: 1) A set of controllers are designed for each operating point (for continuous scheduling parameters, a fine grid is used to obtain a finite set). 2) The controller parameters are interpolated by a polynomial function of the scheduling parameter.

In order to reduce the complexity of the gain-scheduled controller, a linear or low-order interpolation is normally used. In this case, the stability and performance are not necessarily preserved even for the gridded scheduling parameter. The method that we propose puts these two steps together and computes a gain-scheduled controller that satisfies the stability and $H_\infty$ performance conditions for all gridded values of the scheduling parameter using the convex optimization methods. For the ease of presentation, a scalar scheduling parameter and one $H_\infty$ constraint on the weighted sensitivity function are considered. The extension to vector of scheduling parameters and $H_\infty$ constraints on several sensitivity functions is straightforward. In the sequel, the class of models, controllers and design specifications are defined and a convex optimization problem is proposed that results in a gain-scheduled controller.

This research work is financially supported by the Swiss National Science Foundation under Grant No. 200021-121749.

A. Karimi and Z. Emedi are with Laboratoire d'Automatique, Ecole Polytechnique Fédérale de Lausanne, CH-1015 Lausanne, Switzerland. e-mail: alireza.karimi@epfl.ch

### A. Class of models

The class of causal discrete-time LTI-SISO models with bounded infinity-norm is considered. It is assumed that the spectral model of the system as a function of the scheduling parameter $\theta$, $G(e^{-j\omega},\theta)$ is available. The bounded infinity norm condition will be relaxed later on to consider systems with poles on the unit circle. Since only the frequency-domain data are used in the design method the extension to continuous-time systems is straightforward (see [14]).

### B. Class of controllers

Linearly parameterized discrete-time gain-scheduled controllers are considered:

$$K(z^{-1},\rho(\theta)) = \rho^T(\theta)\phi(z^{-1}), \tag{1}$$

where $\phi^T(z^{-1}) = [\phi_1(z^{-1}),\phi_2(z^{-1}),\ldots,\phi_n(z^{-1})]$ represents the vector of $n$ stable transfer functions, namely basis functions vector that may be chosen from a set of generalized orthonormal basis functions, e.g. Laguerre basis [15], and $\rho^T(\theta) = [\rho_1(\theta),\rho_2(\theta),\ldots,\rho_n(\theta)]$ represents the vector of controller parameters. The dependence of the controller parameters $\rho_i$ to $\theta$ can be affine or polynomial, e.g. $\rho_i(\theta) = \rho_{i_0} + \rho_{i_1}\theta + \cdots + \rho_{i_{n_\theta}}\theta^{n_\theta}$.

The main reason to use a linearly parameterized controller is that every point on the Nyquist diagram of the open-loop transfer function becomes a linear function of the vector of controller parameters $\rho(\theta)$:

$$\begin{aligned} L(e^{-j\omega},\rho(\theta)) &= K(e^{-j\omega},\rho(\theta))G(e^{-j\omega},\theta) & (2)\\ &= \rho^T(\theta)\phi(e^{-j\omega})G(e^{-j\omega},\theta), & (3)\end{aligned}$$

that helps obtaining a convex parameterization of fixed-order $H_\infty$ controllers.

### C. Design specifications

The nominal performance can be defined by (see [16])

$$\|W_1 S(\rho(\theta))\|_\infty < 1 \qquad \forall\theta, \tag{4}$$

where $S(z^{-1},\rho(\theta)) = [1+L(z^{-1},\rho(\theta))]^{-1}$ is the sensitivity function and $W_1$ represents the performance weighting filter. The approach proposed in [14] is based on the linearization of this constraint around a known desired open-loop transfer function $L_d$ (that may be a function of $\theta$ as well). The main interest of this linearization is that it gives not only sufficient conditions for the nominal performance but also some conditions on $L_d$ that guarantee the stability of the closed-loop system. The linear constraints are given by [14]:

$$\begin{aligned}&|W_1(e^{-j\omega})[1+L_d(e^{-j\omega},\theta)]| -\\ &R_e\{[1+L_d(e^{j\omega},\theta)][1+L(e^{-j\omega},\rho(\theta))]\} < 0, \forall\omega,\forall\theta \quad (5)\end{aligned}$$

It is easy to show that the inequality in (4) is met if the above inequality is satisfied. Knowing that the real value of a complex number is always less than or equal to its absolute value, we have:

$$\begin{aligned}&|W_1(e^{-j\omega})[1+L_d(e^{-j\omega},\theta)]| -\\ &\quad |1+L_d(e^{j\omega},\theta)||1+L(e^{-j\omega},\rho(\theta))| < 0, \forall\omega,\forall\theta \quad (6)\end{aligned}$$

which leads to

$$|W_1(e^{-j\omega})| < |1+L(e^{-j\omega},\rho(\theta))|, \quad \forall\omega,\forall\theta \tag{7}$$

that is equivalent to (4). Moreover, it can be shown that the number of encirclements of the critical point by $L$ and $L_d$ is equal. As a result, the closed-loop stability is ensured if $L_d(\theta)$ satisfies the Nyquist criterion for all $\theta$ (e.g. it does not turn around -1 for stable plant models). On the other hand, if the plant model and/or the controller have unbounded infinity-norm, i.e. the poles on the unit circle, these poles should be included in $L_d$ (see [14]).

### D. Optimization problem

The constraints in (5) should be satisfied for all $\omega \in [0,\,\omega_n]$, where $\omega_n$ is the Nyquist frequency, and for all $\theta \in [\theta_{\min},\,\theta_{\max}]$. This leads to an infinite number of constraints that is numerically intractable. A practical approach is to choose finite grids for $\omega$ and the scheduling parameter $\theta$ and find a feasible solution for the grid points. This leads to a large number of linear constraints that can be handled efficiently by linear programming solvers. By increasing the number of scheduling parameters, the number of constraints will increase drastically that increases the optimization time. In this case a scenario approach can be used that guarantees the satisfaction of all constraints with a probability level when they are only satisfied for a finite number of randomly chosen scheduling parameters [17]. Some of the effects of gridding in frequency and additional constraints that can be imposed for ensuring good behavior between the grid points are described in [18].

## III. Active Suspension Benchmark

The objective of the benchmark is to design a controller for the rejection of unknown/time-varying multiple narrow band disturbances located in a given frequency region. The proposed controllers will be applied to the active suspension system of the Control Systems Department in Grenoble (GIPSA - lab) [12]. The block diagram of the active suspension system together with the proposed gain scheduled controller is shown in Fig. 1.

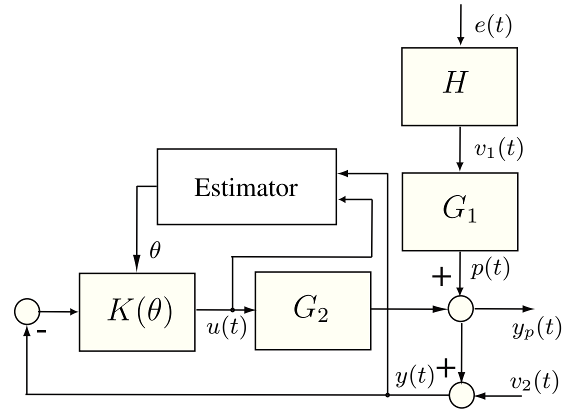

Fig. 1. Block diagram of the active suspension system

The system is excited by a sinusoidal disturbance $v_1(t)$ generated using a computer-controlled shaker, which can be represented as a white noise signal, $e(t)$, filtered through the disturbance model $H$. The transfer function $G_1$ between the disturbance input and the residual force in open-loop, $y_p(t)$, is called the primary path. The signal $y(t)$ is a measured voltage, representing the residual force, affected by the measurement noise. The secondary path is the transfer function $G_2$ between the output of the controller $u(t)$ and the residual force in open-loop. The control input drives an inertial actuator through a power amplifier.

The disturbance consists of one, two or three sinusoids, leading to three levels of benchmark depending on the number of sinusoids. Disturbance frequencies are unknown but lie in an interval from 50 to 95Hz. The controller should reject the disturbance as fast as possible. In this contribution we consider only the first two levels of the benchmark. We explain in detail the control structure and the design method for Level 1. The extension to the second level is straightforward.

### A. Controller design for Level 1

An $H_\infty$ gain-scheduled controller, based on the internal model principle to reject the disturbances, is considered as follows:

$$K(z^{-1},\theta) = [K_0(z^{-1}) + \theta K_1(z^{-1})]M(z^{-1},\theta) \quad (8)$$

where $K_0$ and $K_1$ are FIR filters of order $n$ and $M(z^{-1},\theta) = 1/(1+\theta z^{-1} + z^{-2})$ the disturbance model for a sinusoidal disturbance with frequency $f_1 = \cos^{-1}(-\theta/2)/2\pi$. In order to improve the transient response, the infinity norm of the transfer function between the disturbance and the output, $MG_1S$, should be minimized. However, since the primary path model $G_1$ cannot be used in the benchmark, it is replaced by a constant gain. On the other hand, in order to increase the robustness and prevent the activity of the command input at frequencies where the gain of the secondary path is low, the infinity norm of the input sensitivity function $\|KS\|_\infty$ should be decreased as well. Another constraint on the maximum of the modulus of the sensitivity function $\|S\|_\infty < 2$ (6dB) is also considered according to the benchmark requirements (not to amplify the noise at other frequencies).

The following optimization problem is solved:

$$\begin{aligned} &\min \gamma \\ &\gamma^{-1}\left[|M(e^{-j\omega_k},\theta_i)| + |K(e^{-j\omega_k},\rho(\theta_i))|\right] \\ &\times [1 + L_d(e^{-j\omega_k},\theta_i)]| - \\ &R_e\{[1+L_d(e^{j\omega_k},\theta_i)][1+L(e^{-j\omega_k},\rho(\theta_i))]\} < 0, \\ &0.5|[1+L_d(e^{-j\omega_k},\theta_i)]| - \\ &R_e\{[1+L_d(e^{j\omega_k},\theta_i)][1+L(e^{-j\omega_k},\rho(\theta_i))]\} < 0, \\ &\text{for } k = 1,\ldots,5027, \quad i = 1,\ldots,46 \end{aligned} \quad (9)$$

where the first constraint is the convexification of $\||MS| + |KS|\|_\infty < \gamma$ and the second constraint that of $\|S\|_\infty < 2$.

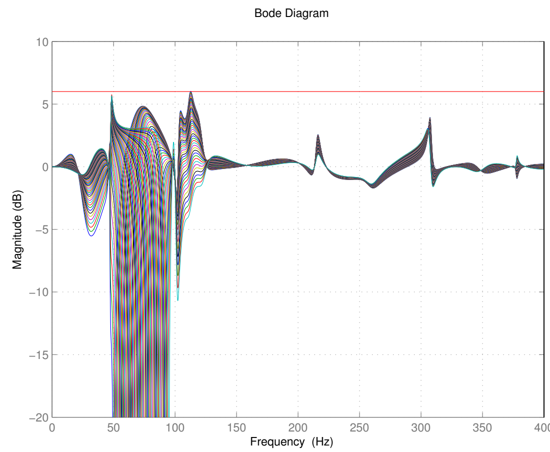


Fig. 2. Magnitude plot of the output sensitivity functions for disturbance frequencies from 50Hz to 95Hz

This is a convex optimization problem for fixed $\gamma$ and can be solved by an iterative bisection algorithm. Because of very high resonance modes in the secondary path model, a very fine frequency grid with a resolution of 0.5 rad/s (5027 frequency points) is considered. The interval of the disturbance frequencies is divided to 46 points (a resolution of 1Hz), which corresponds to 46 points in the interval $[-1.8478\,, -1.4686]$ for the scheduling parameter $\theta$.

**Remarks:**

- The controller order (the order of the FIR models for $K_0$ and $K_1$ in (8)) is chosen equal to 10 which is much less than 26, the order of the plant model.
- The desired open-loop transfer functions are chosen as $L_d(\theta_i) = K_{ini}(\theta_i)G_2$, where $K_{ini}(\theta_i)$ are stabilizing controllers computed by pole placement technique.
- The Frequency-Domain Robust Control Toolbox [13] is used for solving this problem. For the convenience, the internal model is considered as a part of the plant model, i.e. $G(\theta) = M(\theta)G_2$ ,and after the controller design it is returned to the controller.
- After 7 iterations for the bisection algorithm $\gamma_{\min} = 1.68$ is obtained. The total computation time is about 11 minutes on a personal computer.

This gain-scheduled controller gives very good transient performance and satisfies the constraint on the maximum modulus of the sensitivity function for all values of the scheduling parameter. Figure 2 shows the magnitude of the output sensitivity functions $S$ for 46 gridded values of the disturbance frequencies. One can observe very good attenuation at the disturbance frequencies and the satisfaction of the modulus margin of at least 6dB for all disturbances.

### B. Controller design for Level 2

In this level of the benchmark, two sinusoidal disturbances should be rejected. The structure of the gain scheduled controller is given by ($z^{-1}$ is omitted):

$$K(\theta_1,\theta_2) = (K_0 + \theta_1 K_1 + \theta_2 K_2)M(\theta_1,\theta_2) \quad (10)$$

where $K_0, K_1$ and $K_2$ are 8th order FIR filters and

$$M(\theta_1, \theta_2) = \frac{1}{1 + \theta_1 z^{-1} + \theta_2 z^{-2} + \theta_1 z^{-3} + z^{-4}} \quad (11)$$

By considering a hard constraint on the magnitude of the sensitivity function $\|(1 + KG_2)^{-1}\|_\infty < 2.24$ (7dB) the optimization becomes infeasible. Therefore, the following constraint is considered for optimization:

$$|M(1+KG_2)^{-1}|+|(1+KG_2)^{-1}| < \gamma \quad \forall\omega, \forall\theta_1, \forall\theta_2 \quad (12)$$

where $\gamma$ is minimized. Since we have two scheduling parameters a resolution of 1Hz for each sinusoidal disturbances leads to $46^2/2 = 1058$ grid points. This increases by a factor of 23 the number of constraints with respect to that of Level 1. Moreover the resolution of the frequency grid is improved from 0.5 rad/s to 0.2 rad/s which increases the number of constraints. The number of variables is also increased from 22 (the coefficients of two FIR of order 10) to 27 (the coefficients of three FIR of order 8). In order to obtain a faster optimization problem, the scenario approach is used. From the set of 1058 frequency pairs, 50 samples are chosen randomly and the constraints are considered just for these frequencies. The stability of the closed-loop system however, is verified a posteriori for all 1058 frequency pairs. The computed controller, however, destabilized the teal system for disturbance frequency pair (50-70)Hz. The main reason is the modeling error for the secondary path model around 50Hz. Therefore, a new model for the secondary path provided by the benchmark organizers with smaller modeling error around 50Hz is used for the controller design. A new controller is designed using the scenario approach and achieves $\gamma_{\min} = 10.62$ after 11 iterations with a total computation time of about 15 minutes.

The attenuation of at least 40 dB is obtained for all frequencies but the maximum of the output sensitivity function is greater than 7 dB in some frequencies.

### C. Estimator design

The scheduling parameter $\theta$ used in the internal model of disturbance is estimated using a parameter adaptation algorithm. To estimate the parameters of the disturbance model, we need to measure the disturbance signal $p(t)$ (see Fig. 1). If we model $p(t)$ as the output of an ARMA model with white noise as input, we have:

$$D_p(q^{-1})p(t) = N_p(q^{-1})e(t), \quad (13)$$

where $e(t)$ is a zero mean white noise with unknown variance. Estimation of the parameters of $N_p$ and $D_p$ could be performed by the standard *Recursive Extended Least Squares* method [19], if $p(t)$ was measured. Since $p(t)$ is not available, it is estimated using the measured signal $y(t)$ and the known model of the secondary path. From Fig. 1, we have:

$$p(t) = y(t) - \frac{q^{-d}B(q^{-1})}{A(q^{-1})}u(t) - v_2(t), \quad (14)$$

where $\frac{q^{-d}B(q^{-1})}{A(q^{-1})}$ is the parametric model of the secondary path $G_2$. Since $v_2(t)$ is a zero mean noise signal, unbiased estimate of $p(t)$ is given as

$$\bar{p}(t) = y(t)+[A(q^{-1})-1][y(t)-\bar{p}(t)]-B(q^{-1})u(t-d)$$

For the asymptotical rejection of sinusoidal disturbance, there is no need to identify the whole model of the disturbance path, i.e. $HG_1$ as shown in Figure 1. The information needed is just the frequency of the disturbance. So, by setting $D_p(q^{-1}, \theta) = 1 - \theta q^{-1} + q^{-2}$ (for Level 1) and $N_p(q^{-1}) = 1+c_1q^{-1}+c_2q^{-2}$, a simple parameter estimation algorithm can be developed. Let us define :

$$\begin{aligned} z(t+1) &= \bar{p}(t+1) + \bar{p}(t-1) && (15)\\ \psi^T(t) &= [-\bar{p}(t), \varepsilon(t), \varepsilon(t-1)]^T && (16)\\ \Theta^T(t) &= [\theta, c_1, c_2]^T && (17) \end{aligned}$$

where $\varepsilon(t) = z(t) - \hat{z}(t)$ is the *a posteriori* prediction error. Now, the following recursive adaptation algorithm can be used to estimate the the scheduling parameter $\theta$:

$$\begin{aligned} \varepsilon^\circ(t+1) &= z(t+1) - \hat{\Theta}(t)\psi(t)\\ \varepsilon(t+1) &= \frac{\varepsilon^\circ(t+1)}{1 + \psi_f^T(t)F(t)\psi_f(t)}\\ \hat{\Theta}(t+1) &= \hat{\Theta}(t) + F(t)\psi_f(t)\varepsilon(t+1) && (18)\\ F(t+1) &= \frac{1}{\lambda_1(t)}\left[F(t) - \frac{F(t)\psi_f^T(t)\psi_f(t)F(t)}{\frac{\lambda_1(t)}{\lambda_2(t)} + \psi_f^T(t)F(t)\psi_f(t)}\right] \end{aligned}$$

where $\psi_f(t) = \frac{1}{N_p(q^{-1})}\psi(t)$, $\varepsilon^\circ(t)$ is the *a priori* prediction error and $\lambda_1(t)$ and $\lambda_2(t)$ define the variation profile of the adaptation gain $F(t)$. A constant trace algorithm [19] is used for the adaptation gain.

The same recursive adaptation algorithm is used for Level 2 of the benchmark with the difference that $\theta$ is replaced by a vector $[\theta_1\ ,\ \theta_2]$.

## IV. Experimental results

The Experimental results are presented for two different tests of each benchmark level: simple step test and chirp test.

*a) Simple step test:* The experimental results for Level 1 are given in Table I. The first column gives the global attenuation in dB. It is the ratio of the energy of the disturbance in open-loop to that in closed-loop computed in steady state (last three seconds of the experiment). The second column shows the attenuation at the disturbance frequency. The maximum amplification of the disturbance at other frequencies is computed and shown in the third column together with the frequency at which it occurs. The two-norm of the transient response of the residual force is given in the forth column and the two norm at the steady state (last three seconds) in the fifth column. The peak value of the transient response and its duration are given in the 6th and 7th columns.

TABLE III

CHIRP CHANGES

| | Error | |
|---|---|---|
| | **Maximum Value** ($\times 10^{-3}$) | **Mean Square Value** ($\times 10^{-6}$) |
| **Level 1 - Simulation** | 6.40 | 3.5910 |
| **Level 1 - Experimental** | 7.54 | 4.5412 |
| **Level 2 - Simulation** | 10.12 | 10.5170 |
| **Level 2 - Experimental** | 11.56 | 11.8759 |

Figure 3 shows the residual force in closed-loop using the gain-scheduled controller and the scheduling parameter estimator. The transients are greater than that of linear controllers because of the adaptation time of the estimator. Apart from the disturbance at 50Hz, disturbances at other frequencies are rejected and the transient times and their peak values are slightly smaller than those in simulation.

The simulation results for step change of Level 2 are given in Table II. Although, the global attenuation of more than 30 dB was met in simulation for all frequencies, however, in real experiments the performance for the disturbance frequency pair (50-70)Hz is not good. The main reason is that the estimated parameters in the adaptation algorithm do not converge to the true values (a linear controller with known disturbance frequencies performs very well in simulation as well as in real experiments).

*b) Chirp test:* For Level 1 of the benchmark a chirp signal that starts from 50Hz and goes to 95Hz and returns to 50Hz with a variation rate of 10 Hz/sec is applied as the disturbance signal. For Level 2 the disturbance frequencies change from (50-70)Hz to (75-95)Hz with a variation rate of 5 Hz/sec and return to (50-70)Hz. The maximum value and the two-norm of the disturbance response in simulation and in the real-time experiment are given in Table III. The experimental results of the chirp disturbance responses for Level 1 and Level 2 are given in Fig. 4.

## V. CONCLUSIONS

A new method for fixed-order gain-scheduled $H_\infty$ controller design is proposed and applied to the active suspension benchmark. It is shown that multiple unknown sinusoidal disturbances can be rejected using the gain-scheduled controller and an adaptation algorithm that estimates the internal model of the disturbance. The proposed gain-scheduled controller design method is able to satisfy all frequency-domain constraints. However, the results are slightly deteriorated in simulation and real experiments. The main reasons are the followings:

- During the convergence of the scheduling parameter, the whole system becomes nonlinear and the desired performance is not achieved.
- Even at the steady state, there is always an estimation error in the scheduling parameter.
- The modeling error in the secondary-path model is not considered in the design.

It should be mentioned that the proposed method could consider the modeling error in the design and compute a robust controller. However, the unmodelled dynamics makes the optimization method more complicated and lead generally to conservative solutions to the detriment of performance.

## ACKNOWLEDGMENT

The authors would like to thank Prof. Landau for his advices and good discussions and Abraham Castellanos Silva for his help and support during the real-time experiments.

## REFERENCES

[1] K. K. Chew and M. Tomizuka, "Digital control of repetitive errors in disk drive systems," in *American Control Conference*, Pittsburgh, PA, USA, 1989, pp. 540–548.

[2] A. Sacks, M. Bodson, and P. Khosla, "Experimental results of adaptive periodic disturbance cancelation in a high performance magnetic disk drive," *ASME Journal of Dynamic Systems Measurement and Control*, vol. 118, no. 3, pp. 416–424, 1996.

[3] P. Arcara, S. Bittanti, and M. Lovera, "Periodic control of helicopter rotors for attenuation of vibrations in forward flight," *IEEE Transactions on Control Systems Technology*, vol. 8, no. 6, pp. 883–894, 2000.

[4] S. M. Kuo and D. R. Morgan, *Active noise control systems: Algorithms and DSP implementations*. New York, NY, USA: John Wiley & Sons, Inc., 1995.

[5] M. Bodson, A. Sacks, and P. Khosla, "Harmonic generation in adaptive feedforward cancelation schemes," *IEEE Transactions on Automatic Control*, vol. 33, no. 12, pp. 2213–2221, December 1994.

[6] M. Bodson, "Rejection of periodic disturbances of unknown and time-varying frequency," *International Journal of Adaptive Control and Signal Processing*, vol. 19, pp. 67–88, 2005.

[7] H. Du, L. Zhang, Z. Lu, and X. Shi, "LPV technique for the rejection of sinusoidal disturbance with time-varying frequency," *IEE Proceedings - Control Theory and Applications*, vol. 150, no. 2, pp. 132–138, 2003.

[8] P. Gahinet and P. Apkarian, "A linear matrix inequality approach to $H_\infty$ control," *International Journal of Robust and Nonlinear Control*, vol. 4, no. 4, pp. 421–448, 1994.

[9] P. Apkarian, P. Gahinet, and G. Becker, "Self-scheduled $H_\infty$ control of linear parameter-varying systems: a design example," *Automatica*, vol. 31, no. 9, pp. 1251–1261, 9 1995.

[10] Z. Emedi and A. Karimi, "Fixed-order LPV controller design for rejection of a sinusoidal disturbance with time-varying frequency," in *IEEE Multi-Conference on Systems and Control*, Dubrovnik, Croatia, 2012.

[11] M. Kunze, A. Karimi, and R. Longchamp, "Gain-scheduled controller design by linear programming," in *European Control Conference*, July 2007, pp. 5432–5438.

[12] I. D. Landau, T. B. Airimitoaie, A. C. Silva, G. Buche, and M. Noë, "Benchmark on adaptive regulation - rejection of unknown/time-varying multiple narrow band disturbances," *European Journal of Control*, vol. 19, pp. 237–252, 2013.

[13] A. Karimi, "Frequency-domain robust controller design: A toolbox for MATLAB," Automatic Control Laboratory, EPFL, Switzerland, 2012. [Online]. Available: http://la.epfl.ch/FDRC_Toolbox

[14] A. Karimi and G. Galdos, "Fixed-order $H_\infty$ controller design for nonparametric models by convex optimization," *Automatica*, vol. 46, no. 8, pp. 1388–1394, 2010.

[15] P. Mäkilä, "Approximation of stable systems by laguerre filters," *Automatica*, vol. 26, no. 2, pp. 333–345, 3 1990.

[16] C. J. Doyle, B. A. Francis, and A. R. Tannenbaum, *Feedback Control Theory*. New York: Mc Millan, 1992.

[17] G. Calafiore and M. C. Campi, "The scenario approach to robust control design," *IEEE Transactions on Automatic Control*, vol. 51, no. 5, pp. 742–753, May 2006.

[18] G. Galdos, A. Karimi, and R. Longchamp, "Robust controller design by convex optimization based on finite frequency samples of spectral models," in *49th IEEE Conference on Decision and Control*, Atlanta, USA, 2010.

[19] I. D. Landau, R. Lozano, M. M'Saad, and A. Karimi, *Adaptive Control: Algorithms, Analysis and Applications*. London: Springer-Verlag, 2011.

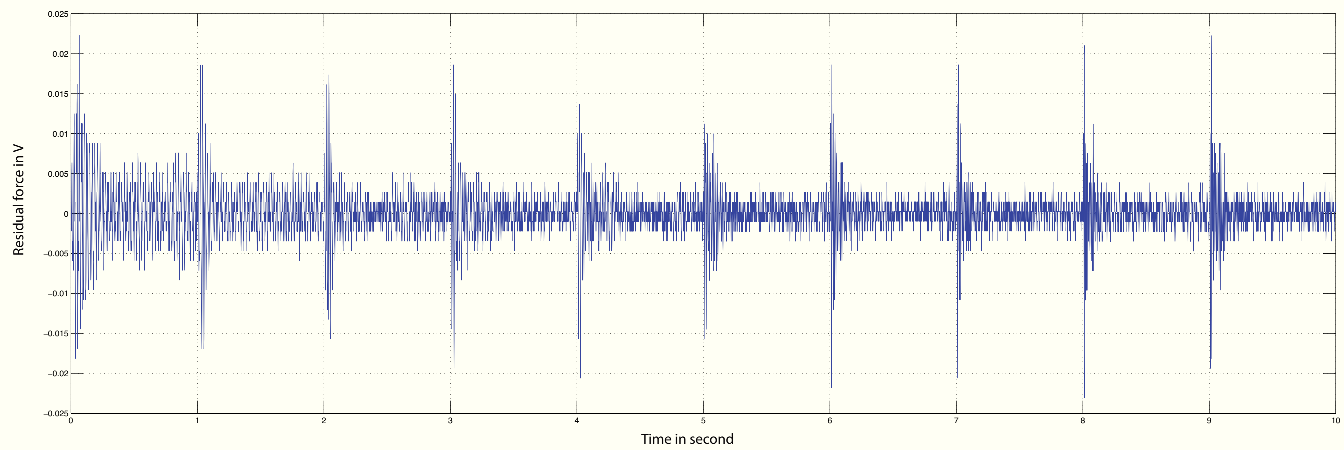


Fig. 3. Transient responses for Level 1 of benchmark in real-time experiment (disturbance frequencies from 50Hz to 95Hz)

TABLE I
SIMPLE STEP TEST (EXPERIMENTAL RESULTS) - LEVEL 1

| **Frequency (Hz)** | **Global (dB)** | **Dist. Atte. (dB)** | **Max. Amp. (dB@Hz)** | **Norm$^2$ Trans.** ($\times10^{-3}$) | **Norm$^2$ Res.** ($\times10^{-3}$) | **Max. Val.** ($\times10^{-3}$) | **Trans. (msec)** |
|---|---|---|---|---|---|---|---|
| **50** | 32.1963 | 26.0390 | 13.19@117.19 | 28.7275 | 9.8031 | 22.2959 | 163.75 |
| **55** | 32.9624 | 41.5091 | 11.66@125.00 | 13.7586 | 5.6248 | 18.5939 | 77.50 |
| **60** | 33.7955 | 41.3196 | 11.59@70.31 | 9.9979 | 5.1623 | 17.3711 | 72.50 |
| **65** | 32.5293 | 45.4435 | 9.54@134.37 | 9.8304 | 5.0178 | 19.3765 | 53.75 |
| **70** | 30.0156 | 42.6926 | 11.41@134.37 | 9.3400 | 5.5506 | 20.6127 | 48.75 |
| **75** | 30.9359 | 43.1902 | 9.74@137.50 | 7.7819 | 4.4682 | 15.7354 | 82.50 |
| **80** | 29.6325 | 44.9083 | 9.43@137.50 | 8.5284 | 5.0297 | 21.8171 | 46.25 |
| **85** | 28.3826 | 38.3824 | 7.63@118.75 | 8.0995 | 5.7268 | 20.5997 | 21.25 |
| **90** | 28.2388 | 37.0264 | 10.02@135.94 | 8.8059 | 5.0778 | 23.0987 | 43.75 |
| **95** | 28.8061 | 37.0992 | 7.36@114.06 | 8.5047 | 4.6892 | 22.2701 | 82.50 |

TABLE II
SIMPLE STEP TEST (EXPERIMENTAL RESULTS) - LEVEL 2

| **Frequency (Hz)** | **Global (dB)** | **Dist. Atte. (dB)-(dB)** | **Max. Amp. (dB@Hz)** | **Norm$^2$ Trans.** ($\times10^{-3}$) | **Norm$^2$ Res.** ($\times10^{-3}$) | **Max. Val.** ($\times10^{-3}$) | **Trans. (msec)** |
|---|---|---|---|---|---|---|---|
| **50-70** | 24.6660 | 20.58 - 17.49 | 18.06@131.25 | 144.4955 | 34.0463 | 50.7286 | 265.00 |
| **55-75** | 36.9297 | 34.20 - 30.54 | 18.88@129.69 | 174.1515 | 6.4665 | 86.2932 | 560.00 |
| **60-80** | 39.9376 | 44.32 - 37.43 | 18.00@134.37 | 64.0941 | 4.0669 | 55.8595 | 393.75 |
| **65-85** | 32.5931 | 37.85 - 32.34 | 14.65@ 135.94 | 47.4775 | 8.2762 | 54.6568 | 200.00 |
| **70-90** | 36.3403 | 55.54 - 47.05 | 14.41@ 137.50 | 52.3746 | 4.7614 | 63.1648 | 250.00 |
| **75-95** | 33.7952 | 43.26 - 36.27 | 13.07@ 137.50 | 116.2289 | 5.7348 | 86.3334 | 410.00 |

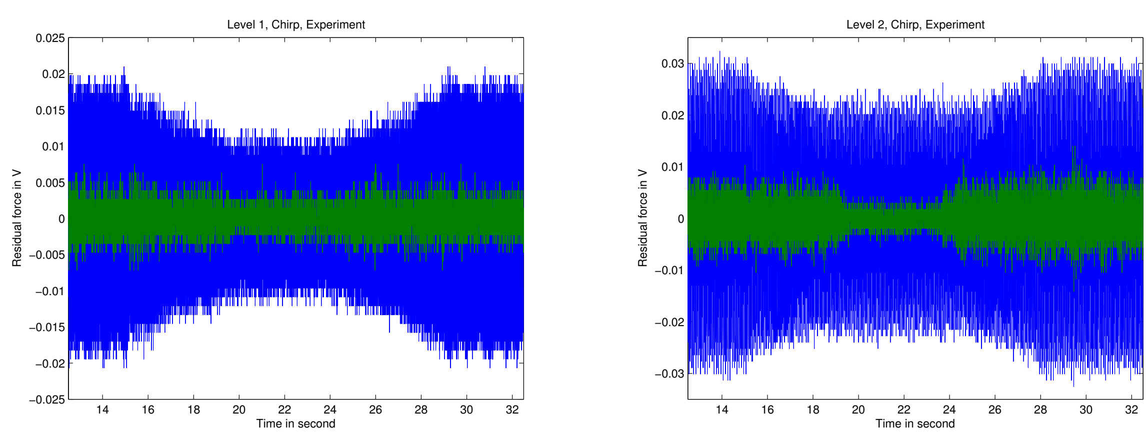


Fig. 4. The experimental results for chirp disturbance responses in Level 1 and Level 2 (open-loop: blue; closed-loop: green)